Synthesis of ZnO/CuO Nanocomposites and Study of their Photocatalytic Properties

By

Hafiz Muhammad Arsalan

Department of Physics
Quaid-i-Azam
University Islamabad
Pakistan.
(2023)

Synthesis of ZnO/CuO Nanocomposites and Study of their Photocatalytic Properties

This dissertation submitted to the Department of Physics, Quaid-i-Azam University, Islamabad, in the partial fulfillment of the requirement for the degree of

Master of Philosophy In
Physics

By
Hafiz Muhammad Arsalan

Department of Physics
Quaid-i-Azam University
Islamabad Pakistan
(2023)

CERTIFICATE

This is to certify that the dissertation entitled **"Synthesis of ZnO/CuO nanocomposites and study of their photocatalytic properties."** by **Hafiz Muhammad Arsalan** submitted to Quaid-i-Azam University, Islamabad for the degree of Master of Philosophy (M.Phil.) in Physics is a record of Bonafede's research carried out by him under my supervision. I believe that this dissertation fulfills part of the requirement for the award of Master of Philosophy. The result embodied in the thesis has not been submitted for the award of any other degree.

Chairman

_____

Prof. Dr. Kashif Sabeeh

Department of Physics
Quaid-i-Azam University
Islamabad, Pakistan

Supervisor

_____

Prof. Dr. Muhammad Shafiq
Professor
Department of Physics
Quaid-i-Azam University
Islamabad, Pakistan

Acknowledgements

All praises and gratitude to the **ALLAH ALMIGHTY**, the most merciful and the most beneficent who showered his countless blessings upon me and give me the courage and knowledge to complete my research work. Countless durood on **HAZRAT MUHAMMAD (PBUH)** whose life is the best source of guidance for us.

I owe gratitude to my discerning supervisor, **Prof. Dr. Muhammad Shafique** for his thought-provoking guidance, patience, motivation valuable suggestions and calm behavior. I am also thankful to **Dr. Abdul Ghafar Wattoo** who helped me to complete this research work. I would like to acknowledge my seniors and lab fellows. I am thankful to my fellows **Shahzad Amin, Mohsin, Javeria Azam and Sana Ishfaq** for their help and cooperation whenever I needed. The good time spent with them can never be erased from my memory.

Hafiz Muhammad Arsalan

Abstract

Treatment of waste water containing organic dyes is very challenging. Photocatalysis can be a viable way to address this problem. Nanocomposites of ZnO/CuO are synthesized in the current study using composite-hydroxide mediated (CHM) approach. The optimal ZnO/CuO composition for the photocatalytic degradation of the methylene blue (MB) is prepared using a variety of compositions. Due to its outstanding catalytic activity and low energy consumption, photocatalytic degradation is one of the most promising methods for removing organic pollutants from our environment. In order to increase the photocatalytic activity for the oxidation of methylene blue, the practical involvement of CuO in ZnO is explored in this study. XRD, SEM, FTIR, and UV-Vis spectroscopy techniques are characterize the synthesized samples. The structural properties reveal that the CuO have a monoclinic phase and ZnO have hexagonal phase structure. According to UV-Vis spectroscopy, all the samples exhibit excellent absorption in the visible spectrum. Increasing the CuO concentration resulted in reduction in the band gap energy from 3.22 eV to 1.73 eV. SEM results shows cotton like surface morphology. The range of particle size lies between 70-200 nm. An FTIR peak observed in 490-600 cm^{-1} shows the formation of metal oxide. Maximum degradation of MB was seen for sample S5, after 150 min which is about 91%.

Contents

List of Figures

List of tables

Chapter 1

Introduction

1.1 Nano science and Nanotechnology

In the recently developed field of nanoscience, materials with extremely small dimensions those on the nano scale are studied. The name nanoscience is a mixture of the words "Nano" which means "Dwarf," and "science," which means information. Controlling and modifying matter at the nanoscale scale is referred to as nanoscience [1]. There is a plenty of room at the bottom is the title of a classic lecture, Professor Richard Feynman gave on December 29, 1959 [2]. The average size of a molecule is a few nanometers, and the diameter of an atom is a few tenths of a nanometer. The human eye cannot see anything smaller than a nanometer. To see a stone in your palm that is 10 nm in size, you would require an eye that is smaller than even a human hair [3]. Nanoparticles are tiny atomic clusters that range in size from 1 to 100 nanometers. Nanoparticles may be crystalline or amorphous, and they can carry gases or liquid droplets on their surfaces. Due to their unique characteristics, such as quantum size and huge surface areas, nanoparticles should be regarded as a separate state of matter in addition to the gaseous, liquid, solid, and plasma states. Nano is a Greek word meaning “dwarf”. According to the National Nanotechnology Initiative (NNI), Nanoscience and Technology (NST) are currently the most discussed areas of study in any creative research institution. Nanoscience is an area of applied science that studies the structure of matter on an atomic or molecular size, usually 100 nanometers or less. It is known to be the environment that can provide answers to many of society's problems in its broadest meaning (nano is the unit of count equal to 10^{-9}) Nanotechnology is a discipline of technology that creates gadgets or materials in this range. According to the National Science Foundation of the United States of America, the nanotechnology market is predicted to reach US$ trillion by 2011. Nanotechnology is evolving engineering self-control that applies techniques from Nano science to the development of practical, marketable, and economically viable goods. Nanotechnology uses the expertise of nanoscience and applies to several fields, though nanoscience only includes the analysis and observation of nanoscale ingredients. Nanotechnology is an engineering arena that operates and uses nanoscale objects for the creation of different useful items. Nanotechnology is precise as use of technical information

to operate and organize substances in nanoscale to take advantage of size and configuration structure-dependend characteristics, configuration and the phenomena different from discrete atoms, molecules, or people associated with bulk materials. ; Material Absorption and control of materials with dimensions of 1–100 nanometers, unique phenomena allow new uses design, development shape and implementation of structures, systems and devices, design, systems and devices by regulating shape unit with precise conditional properties [4].

1.2 Physical Properties of Nanomaterials

Materials at nanoscale, suddenly display different characteristics from those they do not show at the macroscale, opening up new possibilities for study. As an example, copper, which is normally opaque, becomes translucent. Platinum, an inert substance, becomes a catalyst. Aluminum, a stable substance, starts to burn. Insulators made of silicon may become conductors. Gold, which is rigid, stable, and yellow at the micro scale, is liquid and red at the nanoscale. Furthermore, it develops strange catalytic properties that are invisible at macro scale.

1.3 Classification of nanoparticles

1.3.1 Zero-Dimensional NMs

Smooth particle arrangements, heterogeneous particle collections, core-shell quantum dots, hollow spheres, as well as nano lenses are examples of 0D NSMs. Because of their conductivity qualities and specific optical features, 0D nanomaterials are used as a significant probe to raise the sensitivity of biosensors and hence increase their analytical efficiency. Furthermore, 0D NMs, for example, have been intensively researched in (LEDs).

1.3.2 One-Dimensional NMs

Because of their relevance in research and development and vast range of prospective applications, 1D NSMs have sparked a surge of interest during the last decade. It is widely agreed that 1D NSMs are appropriate systems for researching It is widely agreed that 1D NSMs are appropriate systems for researching the size and dimensionality dependency of efficient properties at the nanoscale and exploring a wide range of unique phenomena at the nanoscale. They are predicted to show an essential role as both interrelates and critical units in the fabrication of nanoscale electrical, optoelectronic, and EED devices. Following

Iijima's pioneering work, the field of 1D NMs for example, nanotubes have gained substantial devotion nanotubes have gained substantial devotion.. 1D NMs have a major effect on nanoelectronics, systems, and nanodevices, nanocomposite materials, renewable energy sources, and national security. 1D NMs generated in our and other laboratories, for example, nanowires, nanotubes, nanorods, nanoribbons, classified nanostructures.

1.3.3 Two-Dimensional NMs

Due to its several low dimensional qualities that differ from their bulk properties, Synthetic 2D NMs has become a focal point in materials research in recent years. 2D NMs are synthesized by laser pyrolysis, (CVD), and hydrothermal process. Significant research interest has been spent on the production of 2D NMs in the search for 2D NMs over the last a small number of years in the hunt for 2D NMs. 2D NSMs through specific geometries display distinct shape-dependent properties and can thus be used by way of building blocks in the favor of essential aspects of Nano devices. Furthermore, 2D NMs are predominantly fascinating not merely for simple considerate of nanostructure development mechanisms, 2D NMs are predominantly fascinating not merely for simple considerate of nanostructure development mechanisms but also for the exploration and growth of innovative applications in sensors, Nano containers, and photo catalysts. We show the 2D NMs, like junctions, Nano plates, Nano prisms, Nano sheets, and Nano disks Nano walls.

1.3.4 Three-Dimensional NMs

Because of their huge definite surface area plus other higher qualities over their bulk counterparts due to the quantum size influence, 3D NMs have piqued curiosity of researchers, and several 3D NSMs has been synthesized in last ten years. It is well understood that the behaviors of NSMs are greatly influenced by their sizes, forms, dimensions, and morphology, which are thus critical elements in their which are thus critical elements in their eventual efficiency and applications. As a result, creating 3D NMs with a regulated structure and morphology is of significant interest. Furthermore, 3D NS are an essential material due to their diverse uses in catalysis, magnetic materials, and battery electrode materials. (H. Chen et al., 2009). Furthermore, 3D NSMs have lately piqued the interest of researchers since the nanostructures have a larger surface area provide sample absorption puts for all relevant compounds in a short space. On other hand, such substances with porosity. But from the other hand, such materials with three-dimensional permeability may result in better molecular movement 3 dimensions might lead to a best transference of molecules [5].

1.4 Metal oxide nanoparticles

Due to their tiny size, metal oxide Nanomaterials may exhibit outstanding physical, structural, electrical, and chemical capabilities. When the size of the nanoparticles is reduced, there is an increase in the surface-to-volume ratios. When a nanoparticle's size is reduced only slightly, a large number of the constituent atoms may be located close to its surface, which makes the particle very reactive and donated with exceptional physical capabilities. In the creation of sensors, electrical circuits, fuel cells, piezoelectric devices, layering to protect surfaces from corrosion, and as catalysts, metal oxide nanoparticles may be employed [14].

1.5 **Photocatalysis and Its Significance**

Photocatalysis is the term used to describe the stimulation of a process under the influence of light. Photocatalysts are made of semiconductor metal oxides. Due to their many potential uses in the field of environmental protection, including the remediation of hazardous waste and the treatment of waste water, these materials are particularly fascinating. The creation of an electron-hole pair is the fundamental working principle of a photo catalytic process. Electron-hole pairs diffuse to the photo catalyst's surface and join electron donor and acceptor in the chemical reaction when it is irradiated by light. The neighboring oxygen and water molecules are strongly oxidized by the free electrons and holes to produce OH free radicals. Photocatalysis differs in detail in terms of reactions and mechanism. In first step light is absorbed to produce electron-hole pairs. These exited charges are separated and shifted towards the surface of photocatalyst, where a redox reaction takes place which helps to break the functional bond of any organic dye. Remedial action is required to address the current environmental problem of freshwater contamination like organic pollutants (dyes) in the form of chemical waste. These chemical contaminants are very hazardous and bad for the ecosystem as a whole. Degradation of these organic pollutants is thus necessary to reduce the dangers to human health. So nanocomposites are more effective in the degradation of organic pollutant like methylene blue dye in the presence of sunlight. This research is anticipated to help in the production of high-performing nanocomposites with good photocatalytic activity when exposed to sunshine, which is a free and limitless source of radiations method for treating dye effluents. The discharge of colored effluent from the textile industry into water including lakes, seas, and rivers has generally resulted in serious environmental issues. The majority of colored effluents are poisonous and may cause cancer,

making them a hazard to human existence. Although many chemical and physical procedures have been used to remove colored effluents, such techniques don't completely destroy the dyes. In addition, because the pollution is just changed from one phase to another by the standard operating procedures, further treatment is also needed. The operating cost will subsequently increase as a result. Table 1.1 lists a few benefits and limitations of existing pollution-removal systems [11]. In contrast to conventional methods, the creation of hydroxyl radicals (•OH), which quickly and non-selectively breakdown a variety of pollutants, has improved the degradation of organic compounds. The most recent demanding technique among AOPs seems to be semiconductor Photocatalysis. Photocatalysis offers several noteworthy advantages. Firstly, eliminate the need of mass transfer, streamlining the process. Additionally, its ability to operate in a natural environment. Another key benefit lies in its potential to fully convert organic carbon into carbon dioxide. Moreover, photocatalysis stands out for its affordability, making it cost effective option. Furthermore it is nontoxic.

Table 1.1 Advantages and disadvantages of different techniques for degradation of dye

Method	**Advantages**	**Disadvantages**
Coagulation / Flocculation	Low-cost method	Sludge generation
Oxidation	Fast process to remove Toxic pollutants.	Expends large amount of energy as well as generates by-products.
Electrochemical process	Rapid process as well as effective for certain metal ions	High energy usage.

Irradiation	Useful at laboratory stage.	A large amount of dissolved O_2 is required.
Biological treatment	Feasible in removal of some metals.	Its technology is yet to be established and commercialized

1.5.1 **Photocatalytic Application**

Freshwater contamination caused by leftover organic dyes from several sectors, including textile, pharmaceutical, pesticide, tannery, craft bleaching, cosmetic, food processing, and agricultural, has recently become a significant environmental problem. Figure 1.1 Illustrations of freshwater contamination brought on by chemical spills. In actuality, more than 10-15% of the approximately 7×10^5 tons of organic dyes generated yearly globally are lost to wastewater during production and processing. In addition to being very poisonous and dangerous to living things, these substances also have intermediates that, if not blocked, may engage in reductive reactions that might produce molecules that are carcinogenic. Since these dyes have the potential to be poisonous to the environment, it is imperative that they are remedied right away before being released into the environment. Various techniques have been created in the past to lessen the negative effects that such harmful chemical pollutants have on the aquatic environment, non-human and human life. Adsorption, membrane separation, and biological treatments are some of the less effective removal techniques because of their high operating costs. As an efficient and cost-effective method to get rid of these pollutants, photo degradation technologies based on photo catalytic reactions have recently been developed. Semiconductor nanoparticles (ZnO, SiO_2, and TiO_2) showed excellent potential in this area for photo catalytic applications to remove environmental contaminants [7]. Numerous studies have shown that improving the physical characteristics of nanoparticles with broad surfaces and changed band gaps when they are manufactured, will contribute in boosting the amount of active sites and accelerating

Figure 1.1 Effect of dye contamination on living things [6].

charge transfer which will enhance the photocatalytic activity [8].

1.6 Dyes and their Applications

A dye is a colored substance that chemically bonds to the substrate to which it is being applied.The substances which are used to enhance color, might be artificial or natural. The substrate on which they are put has an affinity for them. Natural (produced from plant sources) and synthetic dyes (man-made) are also acceptable. The creation of consumer goods, such as paper, textiles, paint, printing inks, and paper, predominantly uses dyes. These dyes are disposed of inappropriately in the environment, which has an impact on both plants and animals as well as people. The anhydrous form of methylene blue, seen in Figure 1.2 has a relative molecular mass of 319.85g/mol. It is a solid, flavorless, dark green powder at room temperature that dissolves in water to produce a blue solution. It has a density of 1.0 g/mL at 20°C and a melting point between 100 and 110°C [9]. Methylene blue may be released into the environment via many waste streams as a consequence of its manufacture and usage as a cosmetic and paper dye.

- Methylene blue may be used as a biological dye.
- A redox indicator in analytical chemistry.
- A colorant for paper, leather and clothes.
- A temporary hair dye.

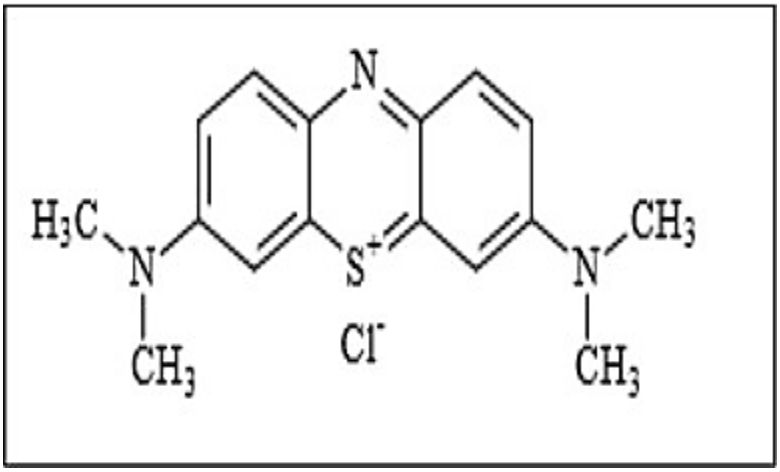

Figure 1.2 Structure of methylene blue.

Methylene blue (MB) may have quite damaging effects on living cells. Humans may experience symptoms such as breathing difficulty, vomiting and diarrhea. Dizziness, headaches, and upset stomach may occur when too much methylene blue dye comes into contact with people. Serious long-term consequences of MB on people include chest discomfort and disorientation. Dye is poisonous and may cause cancer. Even trace levels of dyes present in water bodies have an impact on the environment's quality and clarity of the water bodies. Because these dyes reduce light penetration and reduce photosynthetic activity, which leads to a shortage of oxygen, this results in the extinction of aquatic life [10].

1.7 Advanced oxidation processes

Advanced oxidation processes (AOPs) were first suggested for drinking water treatment in the 1980s and were later extensively researched for the treatment of various wastewaters. Advanced oxidation processes are defined as the oxidative degradation processes involving the generation of highly reactive hydroxyl radicals (OH•), hydrogen peroxide (H_2O_2) and

superoxide anion radicals ($O2^{\bullet-}$) in sufficient quantity to enhance water purification process. AOPs are mainly used for the degradation of organic or inorganic pollutants in water and wastewater. When AOPs are used for water purification, these radicals, as an effective oxidizing agent, are intended to adequately degrade and turn wastewater toxins into minimal and even non-toxic materials, while providing the ideal solution for wastewater treatment. The Environmental Protection Agency (EPA) has approved the introduction of AOP as the recommended technology to meet the criteria with stipulations that deliver secure and effective control of industrial operations and decontamination of contaminated sites [13].

1.8 Basic Principle of Heterogeneous Photocatalysis

Light and the photocatalyst interact in this process. If the energy of the photon is greater than or equal to the semiconductor's band gap (E_g), series of electron and hole pairs will be generated [15].

Photocatalyst + hv → e^- + h^+ (Light absorption)

Because of light interaction, movement of electrons takes place from valence band (VB) to conduction (CB) band with the formation of holes (h^+) in the valence band simultaneously as shown in Figure. These generated charges when reach at surface of semiconductor interact with the surface of methylene blue. Electrons produced by irradiation could easily be trapped by O_2 absorbed on the surface of the photocatalyst or dissolved O_2 to generate superoxide radicals [16].

e - + O_2 → $O_2^{\bullet-}$ (electron conversion)

At the same time, photo induced holes could be captured by surface hydroxyl groups on the photo catalyst surface to create hydroxyl radicals. The oxidation of OH by holes is shown in equation [17].

h^+ + OH^-→ $OH^\bullet$ (hole conversion)

$O_2^{\bullet-}$ could react with H_2O to produce hydroperoxyl radical ($H_2O^\bullet$) and hydroxyl radical ($OH^\bullet$), these radicals are powerful oxidizing agents to degrade the organic molecules [18].

$O_2^{\bullet-}$ + H_2O → $HO_2^\bullet$ + $OH^\bullet$

However, both on surface and in bulk of photo catalyst, photo generated charges (e - and h+) also appear to combine and dissipate heat and could come back to non-excited states.

$e^- + h^+ \rightarrow$ heat **(recombination)**

In this process e^- and h^+ are strong reductive and strong oxidizing agents respectively. Electrons carry out reduction while holes are responsible for oxidation[19].

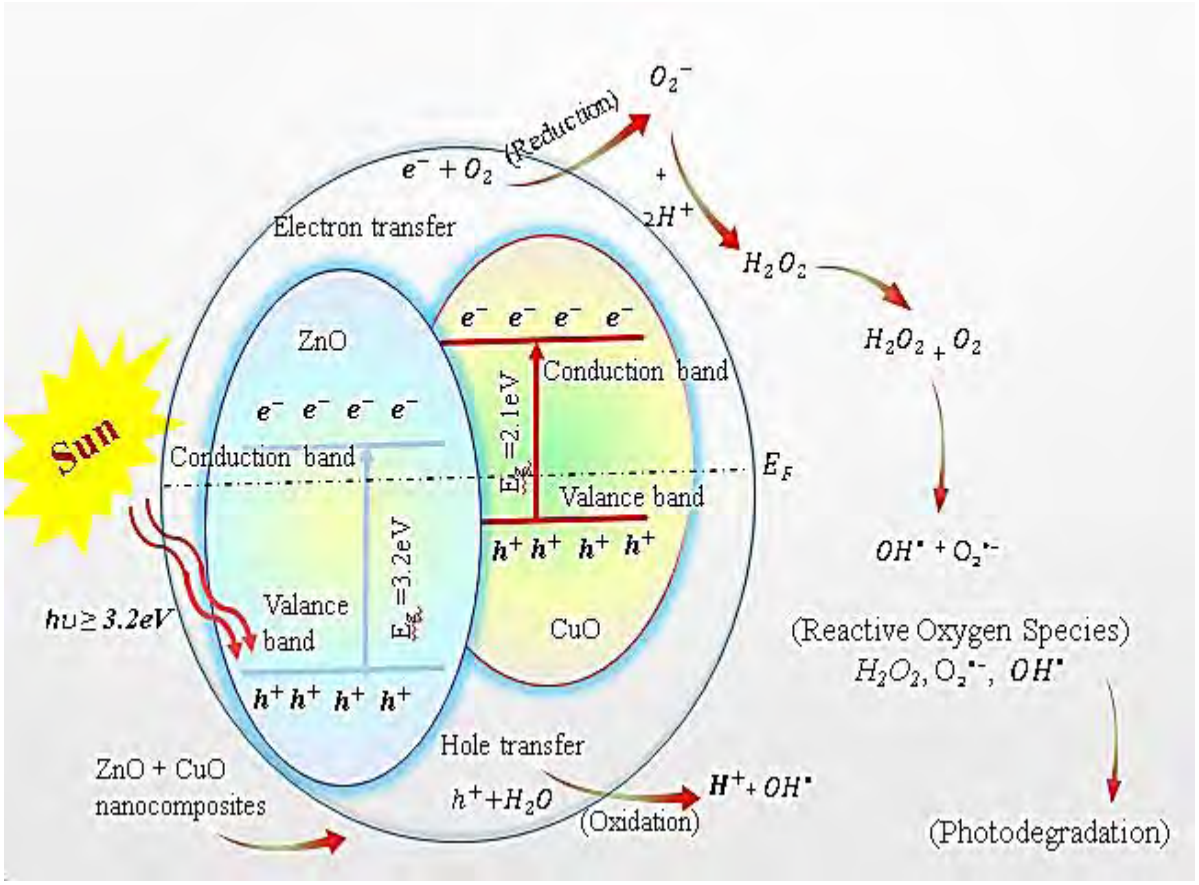

Figure 1.3 Schematic representation of heterogeneous photocatalysis and main reactions taking place on catalyst surface [16].

1.9 Layout of the dissertation

This dissertation is arranged as follows a brief introduction of Nano particles and their photocatalytic properties are presented in chapter 1. Chapter 2 describes dyes, photocatalysis and literature review. Third chapter descries the method for the synthesis of ZnO/CuO Nano composites. Chapter 4 discusses about results obtained from our prepared samples. The structural parameters have been found from X-ray diffraction, surface morphology is studied from scanning electron microscopy, associated functional bonds with our material have been found by Fourier transform infrared spectroscopy technique, The band gap energy of all the samples have been found by Tauc plots, Photocatalytic degradation of methylene blue was evaluated with the help of UV-Vis. Spectroscopy Experimental results of XRD, UV-Visible spectroscopy and SEM are discussed. In chapter 5 conclusions drawn from these experimental results are discussed.

Chapter 2

Literature Review

2.1 Methylene blue removal technique

This includes the photo catalytic approach that concentrates on fully oxidizing organic chemicals into byproducts like water and carbon dioxide. AOPs are used to create hydroxyl free radicals (OH-), which are powerful oxidants that may be used to degrade substances that are resistant to being oxidized by conventional oxidants [20].

2.2 Methods for Improving Photocatalyst Performance

Pure semiconductor photocatalysts biggest flaw is that they have a wide band gap, which implies that high energy and short wavelength photons are needed to jump the valence electron to conduction band. The ultraviolet region of photons is required for this activity. The problem is that just 5 percent of the solar spectrum is made up of UV radiation, whereas 40–45 percent of solar light falls within the visible spectrum. Since UV light is scarcer than needed, photocatalytic activity is constrained. Another significant drawback of semiconductors is the recombination of photo-excited charges, which lowers the procedure's overall performance. The band gap of pure ZnO is high and as UV radiation occupies only <5% of solar rays, it is thus not feasible to use the visible portion of solar energy in a useful way for pure ZnO. The visible light activity of a pure semiconductor photocatalyst must be increased in order to increase its photocatalytic activity. This may be accomplished by altering surface structure chemically, such as doping metals or non-metals, or physically, such as connecting the photocatalyst to other narrow band gap semiconductors. Recombination risks may also be decreased by changes in the crystal structure, such as doping with metals or non- metals, dye sensitization, or the creation of heterostructures [21].

2.3 Factors affecting photo-catalysis

A variety of variables, such as the catalyst's shape, size, and surface area, reaction temperature, pH, light intensity, catalyst amount, and wastewater concentration may affect the rate of photo degradation of an organic molecule. High specific surface area allows for the exposure of more pollutants to hydroxyl radical attack and allows for more pollutants to be adsorbed onto its active surface. Hence by the increase of surface area the photocatalytic

degradation will also increases. By increasing the temperature the rate of photo degradation can be increased. Because higher temperature allows the electron to move from valence band to conduction band which results greater number of electron hole pairs [22]. The light intensity has a considerable impact on how quickly photocatalytic degradation occurs. Higher the light intensity means greater number of photons are available which results in more number of electron hole pairs [23]. The concentration of the catalyst has an impact on the effectiveness of photocatalytic degradation as well. An increase in catalyst leads to an increase in the number of active areas on the surface of the semiconductor, which enhances the formation of OH and O_2 radicals [24].

2.4 Literature Review

In the synthesis of Cu-doped ZnO nanoparticles to degrade methyl orange when exposed to UV light the XRD results showed that Cu-doping prevented ZnO from forming crystals. As Cu2+, the doped Cu element was present. The ideal Cu2+ doping concentration in ZnO is discovered to be 0.5 wt%. The best conditions include calcination at 350 °C for 3 hours to produce 0.5% Cu/ZnO. Over 0.5% Cu/ZnO, the MO degradation rate approaches 88.0%, surpassing that of undoped ZnO. The higher photocatalytic activity of 0.5% Cu/ZnO was primarily driven by the improved charge carrier separation and increased surface hydroxyl groups caused by Cu-doping. The first order reaction was well followed by the photocatalytic degradation of MO kinetics [25]. A basic mechanochemical combustion process is used to prepare CuO/ZnO composites. The produced oxides are characterized using XRD, SEM) and (FTIR). The synthesized CuO/ZnO display a wurtzite ZnO crystal phase and synthesized nanocomposites are made of CuO and ZnO, according to structural analysis. For the degradation of methylene blue (MB) aqueous solution under direct sun irradiation, the photo catalytic capabilities of CuO/ZnO Nano composites are examined. The reactive radicals •O2 and •OH are crucial to the photo degradation of MB. Within 7 hours of exposure to sunshine, MB has mineralized to a level of around 91 percent. The use of sunlight for photo degradation treatment of textile effluent is a simple, affordable method. In contrast to the artificial and costly photo degradation process, the solar photo degradation technology may be a highly efficient way to clean wastewater. Lamp Hg- Xe [26]. ZnO/CuO catalyst nanoparticles were successfully created using the Pechini method of synthesis and the calcination procedure. Investigation and correlation were done on how various temperatures affected functional qualities. The X-ray data demonstrated the creation of the oxides'

distinctive peaks, the growth of crystallites, and improved crystallinity as the temperature rose. Due to the existence of Cu-O and Zn-O bond bands, significant peaks were seen in the infrared and UV-Vis spectroscopy below 500 cm^{-1}. Under sun irradiation, the photo catalytic breakdown of MB was studied. The features shown by the sample that reached 93% MB degradation were then found to be associated with the photo catalytic activity. In order to separate electrons and photo generated holes effectively and provide strong photo catalytic activity, the ratio of Zn and Cu oxides utilized (80:20) may thus be verified. So, it can be said that ZnO/CuO Nano composite is a viable photo catalytic material for the degradation of organic contaminants in an aqueous environment [27]. By using the hydrothermal method, we were able to successfully produce pure ZnO and ZnO/CuO composite. The surface of the ZnO Nano rods has a consistent distribution of CuO nanoparticles, according to the morphological study. Under the influence of visible light, the photo catalytic degradation of MB was studied. The photo catalytic activity shows that ZnO's ability to photo catalyze was discovered to be affected by the presence of CuO. One weight percent of CuO displays improved photo catalytic activity that is ten times greater than pure ZnO at the optimal concentration. In order to digest organic pollutants, ZnO/CuO is thus thought to be a suitable photo catalytic material [28]. Hydrothermal methods have been used to create CuO, ZnO, and CuO-ZnO heterostructures. For the photo catalytic degradation of MB dye under solar light irradiation, all of the samples were assessed. The CuO-ZnO catalyst in sample CZ-1, which resembles a flower, was discovered to be a superb photo catalyst have a capacity of degrading 98 percent of methylene blue in only 30 minutes when exposed to sun light. The benefit of employing solar energy is that no extra power is required, making it particularly cost-effective for processing huge amounts of industrial waste water that contains color molecules [29]. A simple, affordable co-crystallization technique was used to effectively manufacture the ZnO/CuO/g-C3N4 Nano composite. Through visible light illumination, the produced Nano composite was employed to remediate wastewater containing organic contaminants, and the product's robustness and recyclable nature were assessed. The Nano composite’s flawless construction was validated by structural and morphological observations. The ZCG Nano composite had the highest levels of photo catalytic activity, leading to a 97.46 percent photo degradation of MB under visible light in under 50 minutes. By using XRD and FTIR examination of the sample, the ZCG product demonstrated good stability and recycling performance after six consecutive cycles. Overall,

the findings suggest that the ZCG Nano composite might be employed realistically for wastewater treatment that is triggered by visible light, which adds fresh information about catalysts [30]. We have successfully produced pure ZnO and ZnO/CuO nanocomposites composite with various concentrations of CuO for sunlight- induced improved photo degradation activity of organic dye pollution in an aqueous medium. 97 percent of the BCB organic dye was degraded in 100 minutes by ZnO/CuO hybrid nano composites at 5% CuO concentration. The results showed that ZnO's photo catalytic activity was discovered to be influenced by CuO's presence [31]. Organic compounds have been employed as a photocatalyst for the purification of toxic water using zinc oxide, an n-type semiconductor. The use of a p-type semiconductor, such as copper oxide, may enhance catalytic efficiency through the p-n junction by lowering electron-hole recombination. Hand grinding was used to create zinc and copper oxides in this research, which were then heated for five hours at 300°C and contained 1, 3, and 5% copper. SEM, diffuse reflectance, x-ray fluorescence, x-ray diffraction, and x-ray diffraction were employed to examine the zinc oxide and copper oxide mixture as well as their precursors. The direct red 80 tetraazodye decolorization utilizing UV light under pseudo-first order circumstances at natural pH (7.5-8.0) and 30 °C was used to demonstrate the photo catalytic efficiency. The semiconductor containing 1.0 percent copper oxide had the greatest photo catalytic activity; its decolorization rate constant was 6.4010-2 min^{-1}, which is 17.4 percent more than ZnO's 5.45×10^{-2} min^{-1} [32]. It was manufactured a porous octahedral ZnO/CuO hybrid. Porous octahedral particles between 5 and 10 m in size made up the manufactured ZnO/CuO composite. When compared to pure ZnO and CuO, the as-prepared ZnO/CuO composite exhibits better photo catalytic degradation of phenol and a number of dyes in the visible light region The development of a permanent p-n junction in each semiconductors, which effectively divides the photogenerated electron-hole pairs, is what causes the degradation. The porous ZnO/CuO octahedron composite, an active and stable visible- light-driven catalyst, is a potential catalyst for use in the practical treatment of dye pollutants in aquatic effluents [33]. By using two-step hydrothermal techniques, we have described a simple and affordable way to create ZnO/CuO nanocomposites. Under UV illumination, the photocatalytic capabilities of the produced ZnO/CuO nanocomposites has been observed. The findings of the experiments demonstrate that MB may be entirely deteriorated in 15 minutes, and that it has improved photocatalytic activity since its photodegradation percentage is 6 times quicker than pure

ZnO. The improved photocatalytic activity of ZnO/CuO nanocomposites is attributable to the decreased possibility of photogenerated carriers recombining due to the efficient charge transfer between ZnO and CuO [34]. Using an energy-efficient hydrothermal method, we created ZnO-CuO nanocomposites with various ZnO and CuO phase fractions. Using XRD analysis, SEM, and Raman spectroscopy, we looked at the structural characteristics of pure ZnO and ZnO-CuO. Pure ZnO and CuO nanostructures made hydrothermally are less effective in photocatalytic activity tests. According to the computed statistics, the effectiveness of the pure ZnO and CuO nanocomposites was around 24 and 12 percent respectively, after a 120-min photocatalysis time. After keeping in the darkness for 5 hours, the effectiveness was around 25% and 13%, respectively. The photocatalytic activity of nanocomposite samples that included more ZnO phase was more effective. The efficiency of the 76 percent ZnO-24 percent CuO and 67 percent ZnO-33 percent CuO nanocomposites up to 120 minutes was 52 percent and 56 percent separately. After the holding period, these efficiencies considerably increased to 81 percent and 89 percent, respectively, since the photocatalytic process had sufficient time to proceed. But after 120 minutes of lighting and therapy in a dark room, the nanocomposite containing 24 percent ZnO exhibited substantially reduced efficiency of roughly 15 and 20 percent, respectively. Additionally, the mechanical combination, which had the same formula as the best sample (76 percent ZnO + 24 percent CuO), also performed poorly, with efficiency levels of around 26 and 20 percent, respectively. In addition to being highly efficient materials for wastewater cleansing and hydrogen production for energy applications in the future, these distinctive ZnO-CuO Nano composites may offer a new area for photocatalysis study.

Chapter 3

Material and methods

3.1 Method of Synthesis

We have synthesized composites of ZnO and CuO by Composite hydroxide mediated (CHM) technique. Zinc sulphate ($ZnSO_4.7H_2O$), copper sulphate ($CuSO_4.5H_2O$), Sodium hydroxide (NaOH), Potassium hydroxide (KOH) and methylene blue ($C_{37}H_{27}N_3Na_2O_9S_3$) were obtained from Sigma-Aldrich. No further purification was performed on any of the analytical grade compounds before usage. Composite-Hydroxide-Mediated Approach (CHM) technique is adopted for the preparation of ZnO/CuO Nano composites. The CHM technique was used to synthesize ZnO nanocomposites. In this method a metallic salt as source material is reacted with metal hydroxides (NaOH and KOH). Zinc sulphate ($ZnSO_4.7H_2O$) metallic salt was used to synthesize pure zinc oxide. The metal hydroxides serve as precipitating agents to make crystals of ZnO in the following ratio (NaOH: KOH=51.5:48.8). Take a calculated amount of these reactants in a Teflon jar and place it in oven at 170 C^0 temperature. After melting remove this jar and add calculated amount (by doing stoichiometric calculations) of $ZnSO_4.7H_2O$ and place the jar again in oven at 400 C^0 for 24 hours. The vessel was removed and allowed to cool to room temperature after 12 hours of reaction. To get rid of hydroxide on the product's surface, the product was filtered and washed with deionized water. The filtered sample dried in furnace at 40 °C. The dried sample crushed with piston and characterized for further analysis this is the final product named as sample S1. Now to make ZnO/CuO Nano composites repeat the process by adding 10%, 20%, 30% and 40% $CuSO_4$ and named the products as sample S2, S3, S4 and S5. The eutectic point of NaOH/KOH = 51.5: 48.5 is 165ºC, which is chemical equation crucial for synthesizing simple oxides at considerably lower temperature even though the melting temperatures of pure NaOH and KOH are both above 300ºC, m.p of NaOH= 323ºC and m.p of KOH= 360ºC. Hydroxides are essential reactants that reduce the reaction temperature as well as serving as a precipitating agent throughout the reaction process. Fig.3.1 shows the stages involved in making ZnO/CuO Nano composites using the CHM technique.

The reaction process contributing to the generation of pure ZnO and pure CuO is represented in the below.

$$ZnSO_4.7H_2O + 2NaOH + 2KOH \rightarrow 2Zn(OH)_2 + Na_2SO_4 + K_2SO_4 + 14H_2O$$

As $Zn(OH)_2$ is chemically not stable and split to form ZnO and water molecules. The ZnO nanostructures so formed are settled down [36].

$$Zn(OH)_2 \rightarrow ZnO \downarrow + H_2O$$

$$CuSO_4.5H_2O\ 2NaOH + 2KOH \rightarrow Cu(OH)_2 + Na_2SO_4 + K_2SO_4 + 5H_2O$$

As $Cu(OH)_2$ is chemically not stable and split to form CuO and H_2O. So according to the following reaction, the ZnO nanostructures so formed are settled down.

$$Cu(OH)_2 \rightarrow CuO \downarrow + H_2O$$

Figure 3.1 An illustration of the stages involved in the synthesis of ZnO/CuO nanostructures using the CHM technique

3.2 Instrumentation

Scanning electron microscopy SEM, X-ray diffraction (XRD) and Fourier transform infrared spectroscopy (FTIR) were used to characterize a newly created series of modified ZnO photocatalysts. By the above techniques, morphological analysis, chemical composition and crystallite size of synthesized photocatalyst was examined. UV-Vis spectroscopy was utilized to find each sample's optical absorption spectrum during the photocatalytic activity test.

3.2.1 X-Ray Diffraction (XRD)

The X-ray scattering technique is a diagnostic method that helps to find crystallographic structure, chemical composition and physical characteristics of materials. Additionally, it is possible to distinguish between crystalline and amorphous materials using the X-ray diffraction method. The structure is recognized by examining the X-ray diffraction pattern and matching it with the standard powder diffraction files released by the international center for diffraction data (ICDD)). From XRD we investigate the development of a certain material system, calculating the lattice parameters, miller indices, and unit cell structure, determining the phases (crystalline substances) that are present in the material, estimating the sample's crystalline/amorphous composition, determining the breadth of the peak in a certain phase pattern to determine the average crystalline size. Sharp peaks form at large grain sizes. When a monochromatic X-ray impinges on a crystal lattice, every atom in the structure serves as a source for scattering radiation of the same wavelength. The intensity of the reflected beam at a certain angle will be at its greatest when the path difference between two reflected waves from two different planes is an integral multiple of wavelength. Diffraction happens when an X-ray beam impacts a crystal because the wavelength of X-ray beams is equal to the separation between atoms in materials. The bulk of X-ray interactions with the conventional 3-D arrangement of atoms on a crystal are destructive and cancel one another out, but in a certain direction, they are constructive and reinforce one another. Scherrer formula is used to compute the crystalline size (D) from Full Width at Half Maximum (FWHM).

$$D = K.\lambda/(\beta \cos \theta)$$

Figure 3.2 XRD machine

Where D is the average crystalline size in nm, K = 0.9 the shape factor, λ is the wavelength of X-ray (0.01 nm) used, and β is FWHM (full width half maxima) of respective diffraction peak.

3.2.2 UV-Vis. Spectroscopy

When using CCDs, which collect light of various wavelengths on various pixels, diffraction gratings are used. Although gases and even solids may have their absorbance measured, liquids are most often the samples used in UV-Vis spectrophotometers. Typically, samples are put in a cuvette, which is a clear cell. Cuvettes generally have a rectangular form and a 1 cm internal width. The most extensively used cuvettes are UV- visible (UV-Vis) cuvettes, and spectroscopy is used to get the absorbance spectra of a substance in solution. The

absorption of electromagnetic radiation or light energy, which excites electrons from the compound or material's ground state to its initial excited state, is what is really being detected spectroscopically. The UV-VIS region of the electromagnetic spectrum spans 1.5–6.2 eV, or 800-200 nm in wavelength terms. It measures the intensity of light flowing through a sample (I) and contrasts it with the intensity of light preceding the sample (Io). Transmittance, which is often stated as a percentage (%T), is the ratio I/Io. As illustrated in Figure, the essential components of a spectrophotometer are a light source, a holder for the sample, a diffraction grating or monochromator separating the various wavelengths of light, and a detector. The radiation source is often a tungsten filament (300–2500 nm), a continuous deuterium arc lamp for the ultraviolet area (190-400 nm), and more recently light emitting diodes (LED) and xenon arc lamps for the visible wavelengths. Usually, a photodiode or a charge-coupled device serves as the detector (CCD). When used with a monochromator, photodiodes filter the light so that only wavelengths with a certain frequency may reach the detector. With CCDs, which gather light of various wavelengths on various pixels, diffraction gratings are employed. The most typical samples for UV-Vis spectrophotometers are liquids, while it is also possible to measure the absorbance of gases and even solids. Typically, samples are put in a cuvette, which is a clear cell. Cuvettes often have an interior width of 1 cm and are generally rectangular in form. High grade quartz glass cuvettes are the most extensively used since they are clear across the UV, visible, and near infrared spectrums. The relationship between absorbance and route length and absorbing species concentration is direct. The amount of the species absorbing the light dictates how much of it is absorbed, and the maximum wavelength of the absorption band will provide information about the structure of the molecule or ion. On the basis of Beer's Law, which is represented by the equation, quantitative measurements are made.

$$\mathbf{A = \varepsilon \times b \times c}$$

Where **ε** is the constant of proportionality, b is the path length, and c is the concentration of MB [37].

3.2.3 Scanning electron microscopy (SEM)

SEM uses electron to observe objects. It is because of the smaller wavelength of electron as compared to photons to get high resolution images. Basic principle of SEM is that a beam of electrons produces secondary electron from sample surface. Those secondary electrons then form an image to for surface analysis. A beam of electron is formed from electron gun. Electro-magnetic field with the help of condenser lens is applied to condense the ray of the electrons. This ray of electron is then made to fall upon sample surface. A detector is used to collect signals from scattered, auger and secondary electrons to give final image. A clearer idea can be obtained from flow diagram, which describes how the electron beam passes through different stages and finally the formation of highly resolution image of sample is obtained. Instead of visible light, the SEM pictures were produced using transmitted electrons that can achieve magnifications of up to 100000X with a resolution of up to 100Å.

3.2.4 FTIR

The Fourier transform infrared spectrometer is one piece of equipment based on infrared spectroscopy (FTIR). It is now the most popular and modern kind of dispersive spectrometer. Its success may be attributed to several factors, including its high precision, accuracy, speed, enhanced sensitivity, simplicity of operation, and sample non-destructiveness. The basis for infrared spectroscopy is a molecule's atomic vibrations, which only absorb certain infrared frequencies and energies. Because different chemicals have unique infrared spectra, FTIR can distinguish between and categorize them. The FTIR spectrometer really uses an interferometer to detect the amount of energy that is delivered to the sample. The interferometer, which performs signal spectral encoding, receives the infrared light that the black body emits. When an interferogram is produced, certain energy wavelengths are absorbed on the sample surface and the signal passes through or reflects off of it. The beam is eventually sent to a computer for Fourier processing of the energy signal after passing through the detector.

Chapter 4

Results and discussions

4.1 Structural Assessment

All of the nanocomposites' structural properties were determined using X-ray diffraction (XRD). XRD spectrometer operated at 30 KV and 40 m A using Cu-K_α (1.54 A^o).XRD spectra's of S2, S3, S4 and S5 are shown in figure 4.1. The Debye-Scherer formula has been used to determine the crystallite size.

$$\boldsymbol{D = K.\lambda/(\beta\, cos\, \theta)}$$

Where K is Debye constant and its approximate value is 0.9, λ is the wavelength of x- rays and its value is 1.54 Å. β is known as full width at half maximum and can be calculated by the formula:

$$\boldsymbol{\beta}\ \frac{\boldsymbol{FWHM\times 2\pi}}{\boldsymbol{360}}$$

The XRD data was employed for identification of crystal structure, interplanar spacing, crystallite size, dislocation density and calculation of miller indices.

Fig 4.1 shows the typical ZnO major peaks which appeared at 2θ = 34.69^o, 47.67^o, 69.04^o corresponding to the (002), (102), (201). The XRD pattern confirms that the synthesized ZnO nanoparticles belong to the wurtzite hexagonal structure (JCPDS data card No. 00-036-1451). The hexagonal wurtzite phase of ZnO, with lattice constants of a = b = 0.324 nm and c = 0.521 nm, has been identified. And XRD peaks at 2θ = 38.25^o, 45.81^o, 71.28 ^{o}, corresponding to the (111), (-112), (31-2), planes. This XRD pattern confirms the monoclinic structure of CuO (JCPDS data card No. 00-048-1548). With lattice constants of a = 0.468 nm, b = 0.343 nm, and c = 0.513 nm, this pattern has been classified as the monoclinic phase of CuO. Two sets of diffraction peaks for the connected metal oxides can be seen; they are attributed to hexagonal ZnO and monoclinic CuO, demonstrating the effective synthesis of the composite. In S3, one major peak (002) is at same angle shows that d-spacing is same as S2, but second major peak (102) is shifted toward left by 0.29^o indicting that d-spacing is increased and hence an expansion occurred in the lattice. In S4, all three major peaks (002), (102), (201) are shifted towards higher angle indicating that d-spacing is decreased at that angle and a contraction is occurred in the lattice. Similarly in S5 two major peaks (002), (102) are also shifted towards right indicating that d-spacing is decreased and hence contraction occurred in the lattice. A few peaks also appeared which does not matched with any of the JCPDS card of ZnO or CuO which may be due to impurity atoms added from substrate or sample holder.

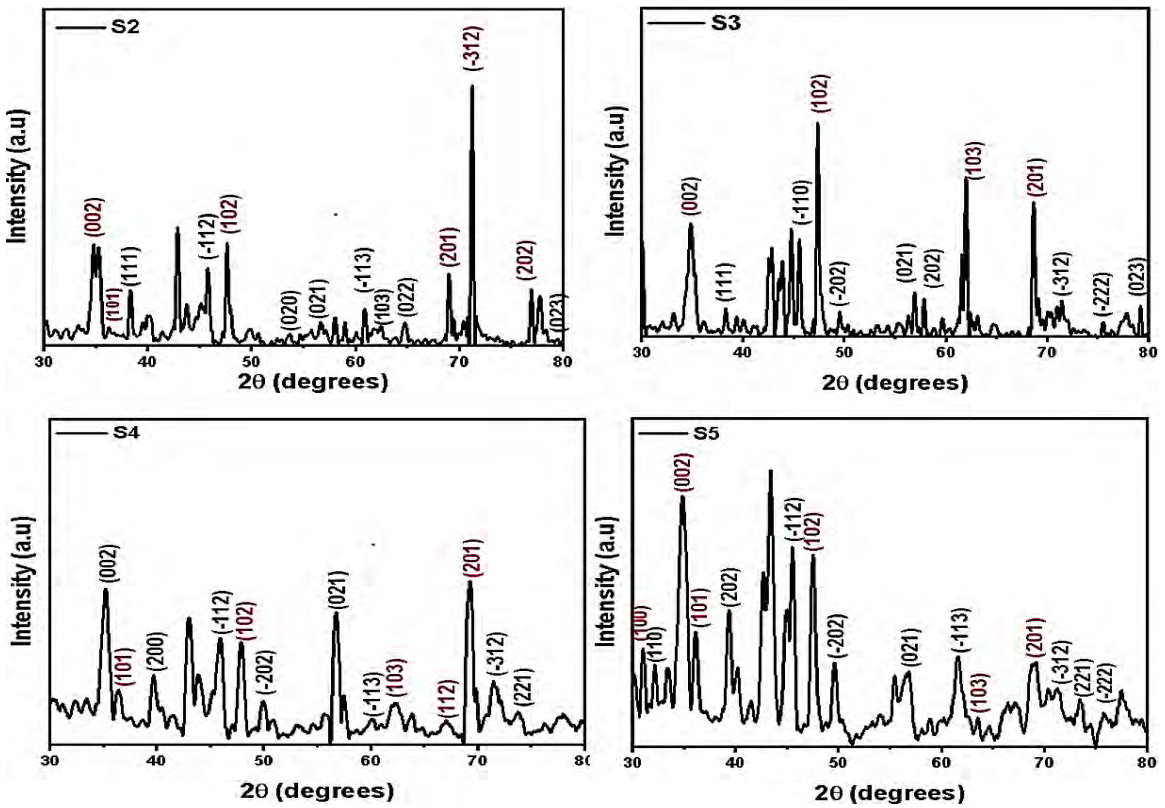

Figure 4.1 XRD patterns of all prepared composites.

. But all major peaks are well matched with [38] which confirms the successful synthesis of our material. The size of the crystallites, which was calculated from the Debye-Scherer formula is shown in Table (2). As the CuO loading raised, the crystallite size goes on decreases which offers more active sites for the interaction between catalyst surface and organic pollutant. The Interplanar spacing increases by the increase of CuO concentration due to small ionic size of CuO molecules, which offers large surface area for the photocatalytic degradation [38].

Table 4.1 Structural parameters of all composites

Samples	Interplanar spacing	Crystallite size	Dislocation density
S2	1.71	23.44	0.00182
S3	1.83	22.42	0.00198
S4	1.95	8.27	0.01462
S5	4.51	8.14	0.01509

4.2 Morphological Analysis

The surface morphology and particle size of each sample were examined using scanning electron microscopy (SEM). Surface morphology and size of nanoparticles play an important role in photocatalytic degradation. SEM is an appropriate technique to study the surface morphology of the samples. The SEM is competent of making large-resolution

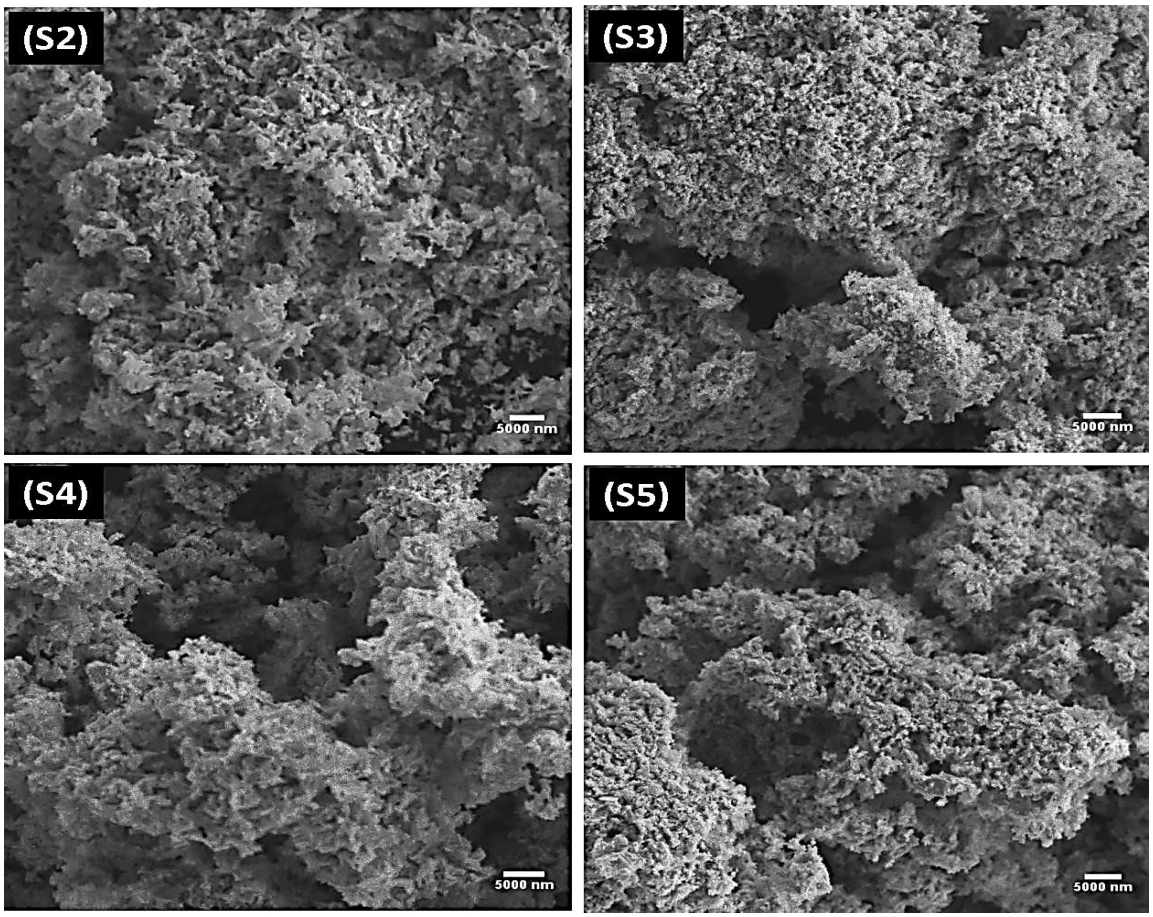

Figure 4.2 SEM images of all prepared composites.

Images of material. In our study, SEM analysis was performed for all the prepared composites. The morphological analysis shows that the particles exhibit cotton like morphology having porous structure which have large surface area for light irradiation. The size of nanoparticles is in the range of 70 to 200 nm. After incorporation of CuO, uniform distribution of CuO on ZnO is observed. When relating the particle size to the crystallite size, it is observed that the particle size is much larger than the crystallite size, which confirms that the synthesis of nanocomposites as active photocatalyst. The surface

morphology of all the composites synthesized by the composite hydroxide mediated method is shown in figure 4.2.

4.3 Fourier Transform Infrared Spectroscopy (FTIR)

Chemical bonds that were discovered in the material were examined using FTIR analysis. Fourier Transform Infrared Spectroscopy (FTIR) produces an infrared absorption spectrum that may be used to identify the chemical bonds inside a molecule. The spectra give samples a profile, a unique chemical fingerprint that may be used to scan and analyse the samples for different ingredients. Every bond or functional group require a unique frequency of oscillation for absorption of light, hence a characteristic peak is observed for every functional group. In our study, FTIR analysis was performed for the prepared samples. FTIR analysis was performed for S1, S2, S3 and S4 respectively. With the use of an FTIR spectrophotometer, Figure 4.3 illustrates the functional groups of Nano scale ZnO, CuO, and CuO-ZnO materials. The alkane groups' C-H stretching vibration, which may have been present due to the environmental variables, is what causes the peaks between 2830 and 3000 cm-1. A frequency of 3500–3000 cm^{-1} allowed the detection of the -OH functional groups [39]. The additional peaks between 839 and 1670 cm^{-1} are caused by the H-O- H molecule's bonds being stretched. The organic molecule created during the synthesis of CuO is thought to be responsible for the absorption band at 2350 cm-1 [40]. The C=O group is responsible for the 1555 cm^{-1} peaks. In the range of 490-600 cm^{-1}, which corresponds to the Zn-O bond, which confirm the formation of ZnO [41].

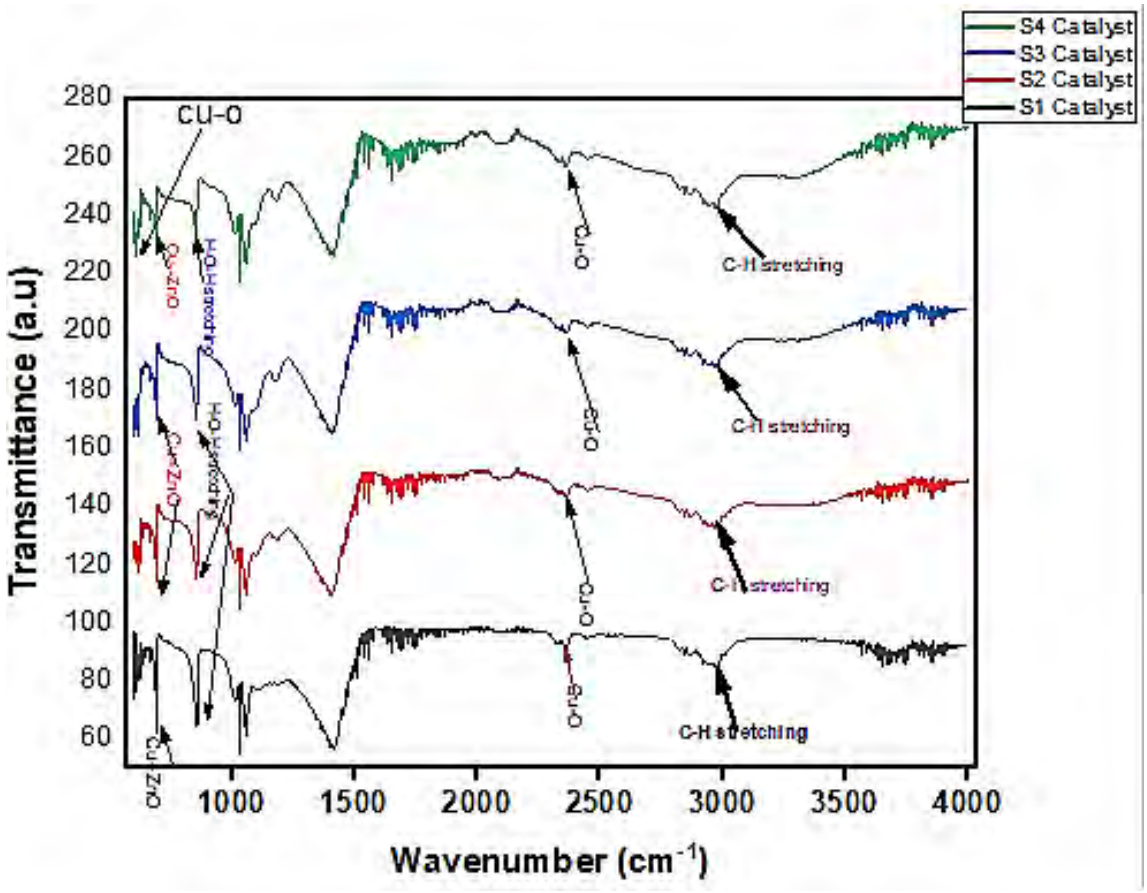

. **Figure 4.3 FTIR Spectra of S1, S2, S3, and S4.**

4.4 Band Gap Calculation

After absorbing the necessary amount of energy, valence band electrons go from the valence band to the conduction band. The relation between absorption spectra and the energy of the band gap is shown by the Tauc equation [42].

$$(\alpha h\upsilon)=k\,(h\upsilon-E_g)^{n}$$

Depending on whether the transition is direct or indirect, n can either be 1/2 or 2, where α is called absorption coefficient, h is planks constant, υ is frequency of light. Band gap energy is denoted by Eg, while constant K is also referred to as the band tailing parameter which depends on index of refraction and electron and hole effective masses, however it usually taken as 1. Using the Beer-Lambert equation (A = α × l× □) the coefficient of absorption (α) is calculated. The value of the band gap E_g is shown by extrapolating the linear area of the figure $(\alpha h\upsilon)^{2}$ vs. energy (hυ). Band gap values may varies depending on the concentration of CuO in ZnO [43]. We have calculate the band gap from the graphs which

are plotted b/w energy (hυ) and $(\alpha h\upsilon)^2$. In figure (4.4), (4.5), (4.6), (4.7) and (4.8) a graph intersects the energy axis at 3.22, 2.48, 2.23, 1.98, 1.73 eV respectively which is the band gap for S1, S2, S3, S4 and S5.

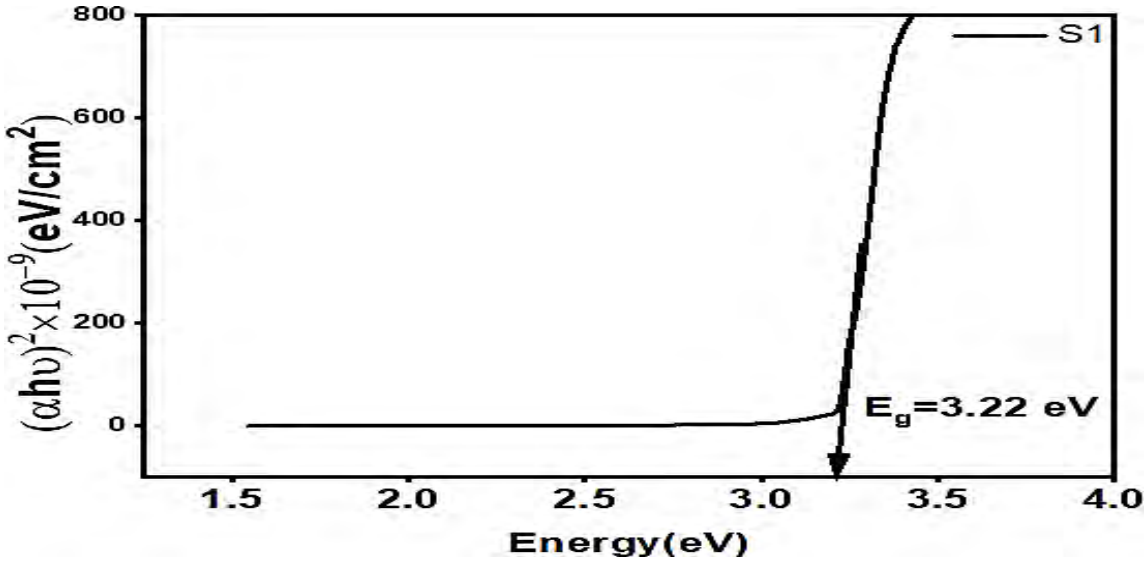

Figure 4.4 (a) Tauc's Plot of S1.

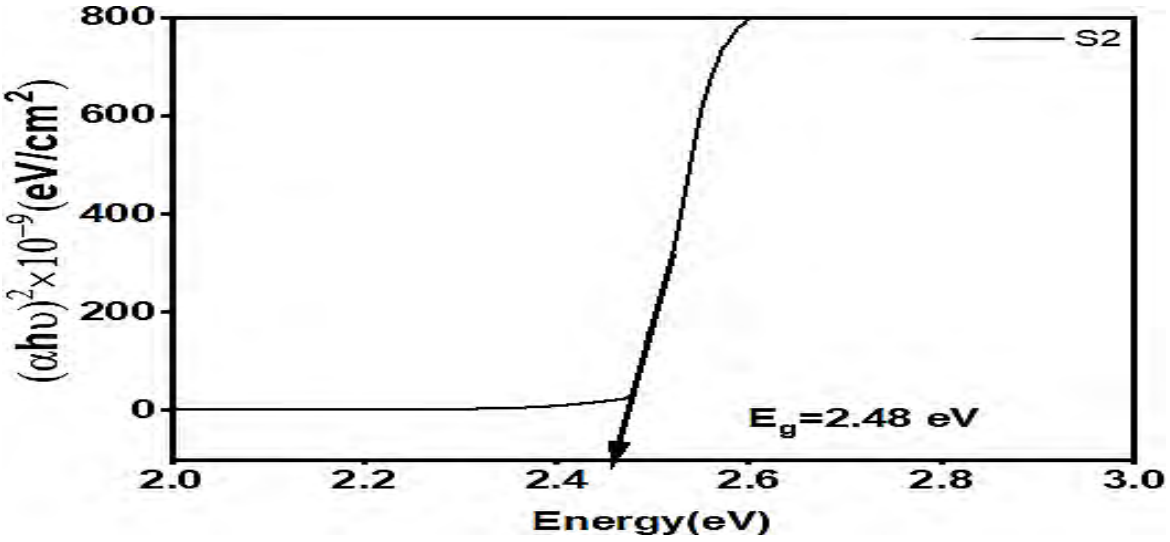

Figure 4.4 (b) Tauc's Plot of S2.

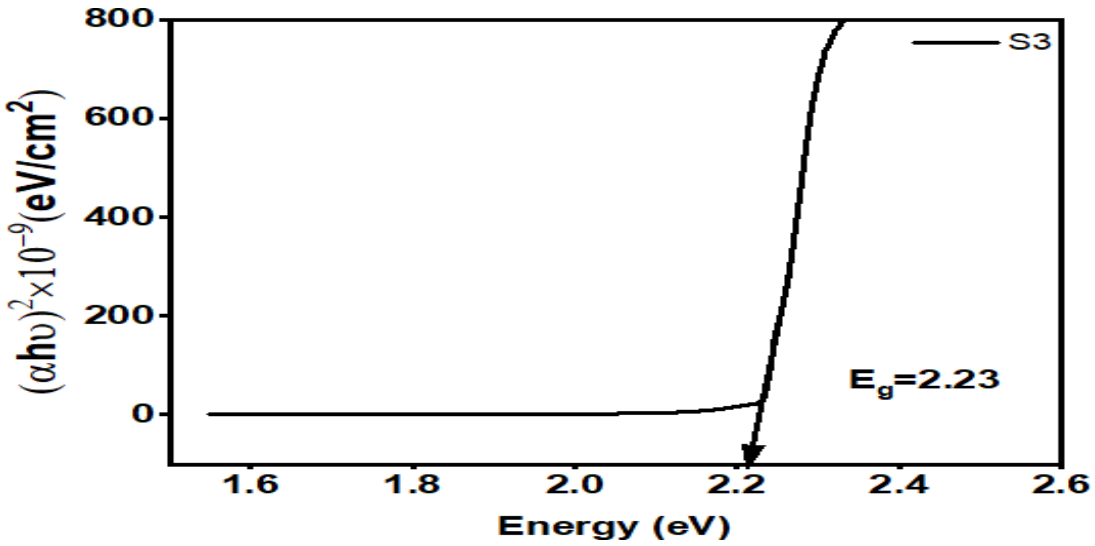

Figure 4.4 (c) Tauc's Plot of S3.

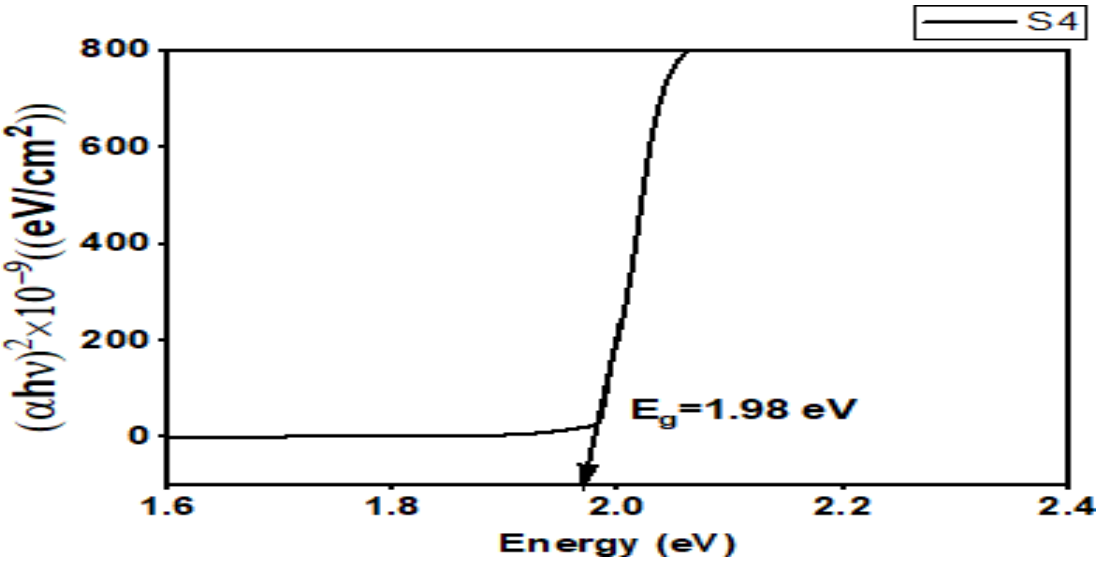

Figure 4.4 (d) Tauc's Plot of S4.

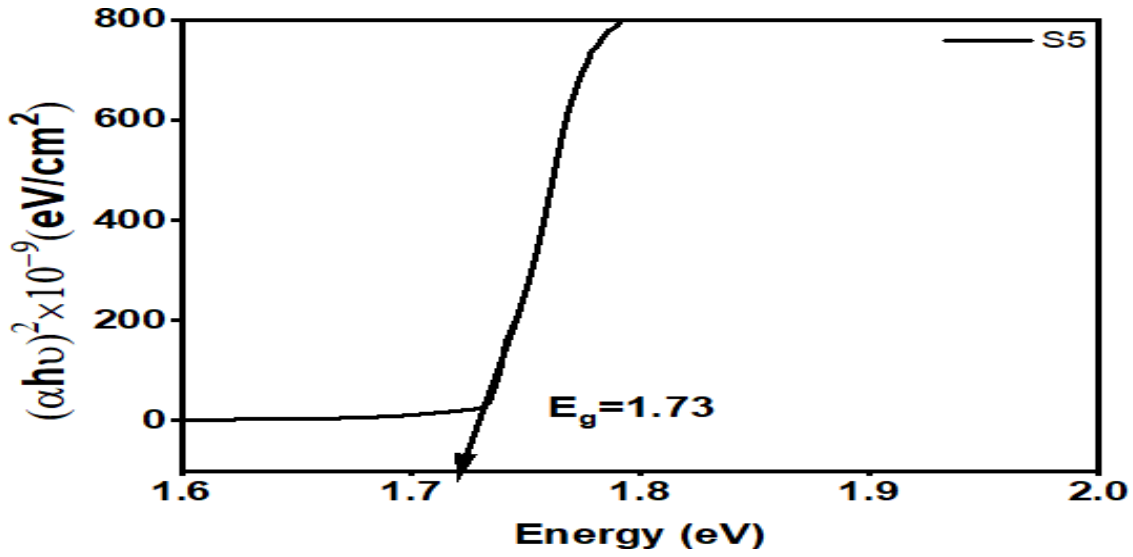

Figure 4.4 (e) Tauc's Plot of S5.

From above figures it has been noted that the coupling of CuO causes the band gap of ZnO to decrease significantly, which results in the motion of electrons from valence band to conduction band, generating the electron hole pairs which leads to the better photo degradation. The comparison of band gaps of synthesized photo catalysts is listed in Table 4.2.

Table 4.2 Band gap of different catalysts

Photo catalyst	Band gap (eV)	Change w.r.t pure ZnO
S1	3.22	0
S2	2.48	0.74
S3	2.23	0.99
S4	1.98	1.24
S5	1.73	1.49

4.5 Photocatalytic degradation of dye

The spectrum of the pure methylene blue by using the UV-vis spectrometer is shown in fig 4.5. The two larger peaks at different wavelengths are observed. Major peak is observed at the wavelength 664 nm with 2.177 (a.u) absorbance which shows maximum absorbance at

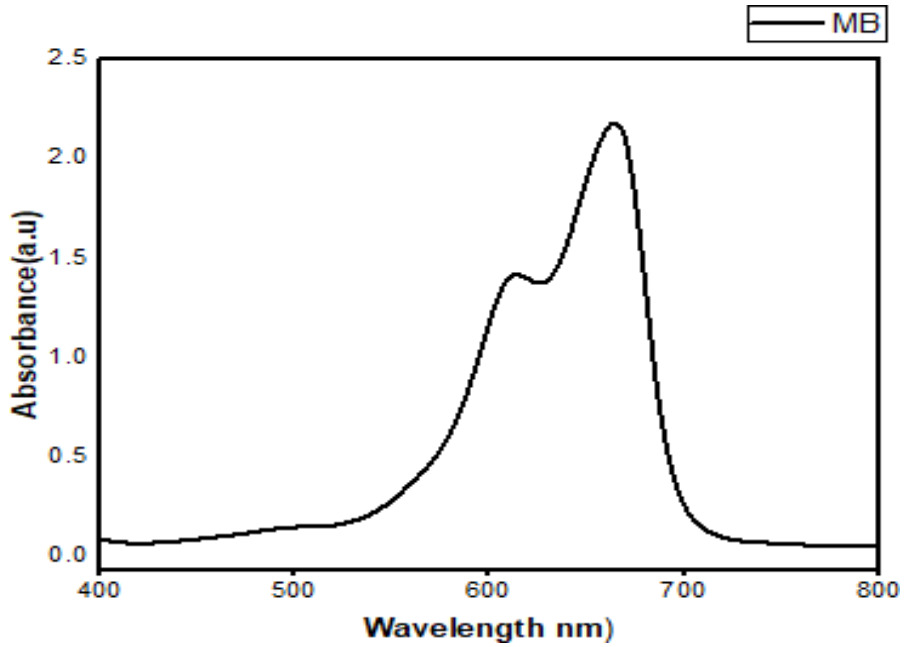

Figure 4.5 MB curve without any catalyst

664 nm, with the passage of time there is no change in the peaks which shows that without catalyst dye molecules cannot be degraded.

4.5.1 Examine the impact of time on methylene blue's degradation

By changing the reaction time between 0 to 150 minutes, the impact of reaction time on the photo degradation of methylene blue using S1 (ZnO) photo catalyst was investigated. Methylene blue solution along with desired photo catalyst amount was kept under the source of visible light. The photo degradation reaction took place under the following circumstances;

- Time: 0 to 150 minutes.
- Catalyst dose: 0.04 g.

- Methylene blue concentration: Kept constant at 12ppm.
  In Figures 4.10, 4.11, 4.12, 4.13 and 4.14 a graph is plotted between absorbance and time for the catalysts S1 (ZnO), S2ZnO) $_{0.90}$ + (CuO) $_{0.10}$, S3 ZnO) $_{0.80}$ + (CuO) $_{0.20}$, S4ZnO) $_{0.70}$ + (CuO) $_{0.30}$ and S5 S_5ZnO) $_{0.60}$ + (CuO) $_{0.40}$ respectively. The graphs shows that when exposure time is increased, the dye solution's distinctive UV absorption peak also quickly falls along with it, which shows that dye molecules are degrading and less molecules are available to absorb light. By extending the amount of time exposed to visible light, the rate of electron transfer from the valence band to the conduction band rises, which also improves photo degradation performance. After 150 minutes methylene blue degradation percentage was

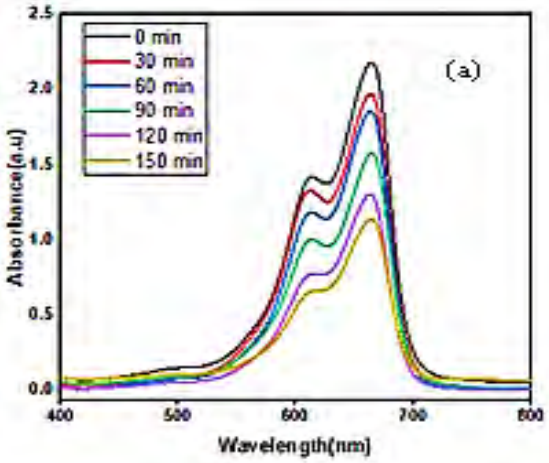

Figure 4.6 (a) Time optimization of S1

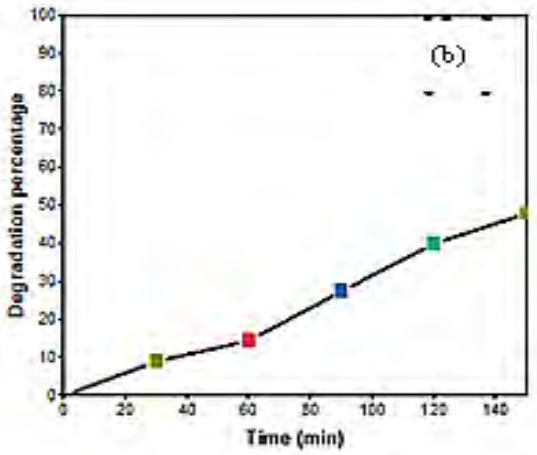

Figure 4.6 (b) Degradation % of S1.

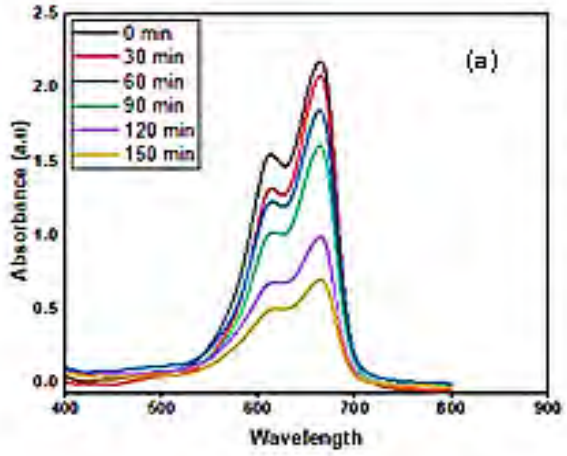

Figure 4.7 (a) Time optimization of S2

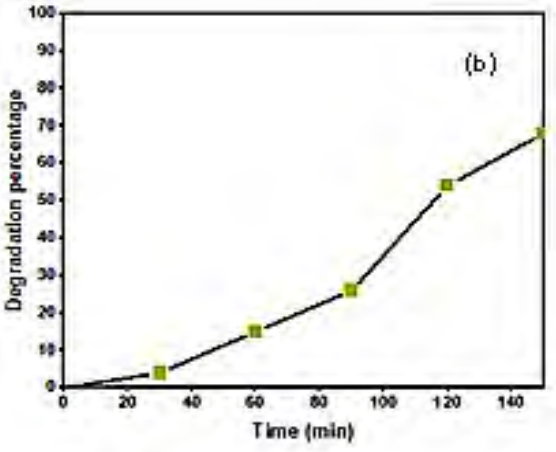

Figure 4.7 (b) Degradation % of S2

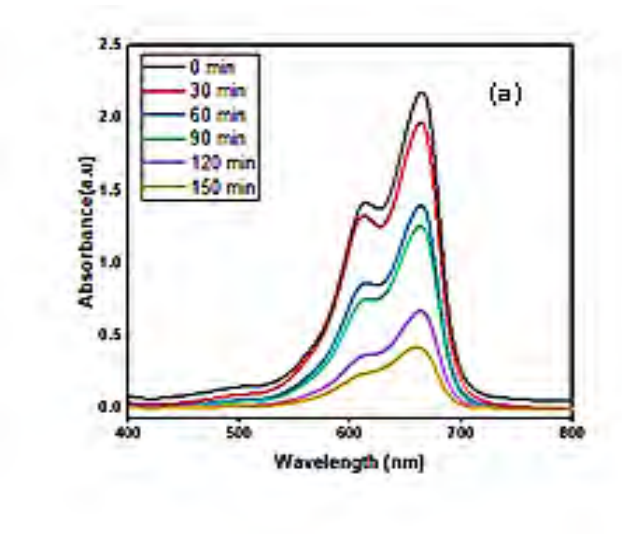

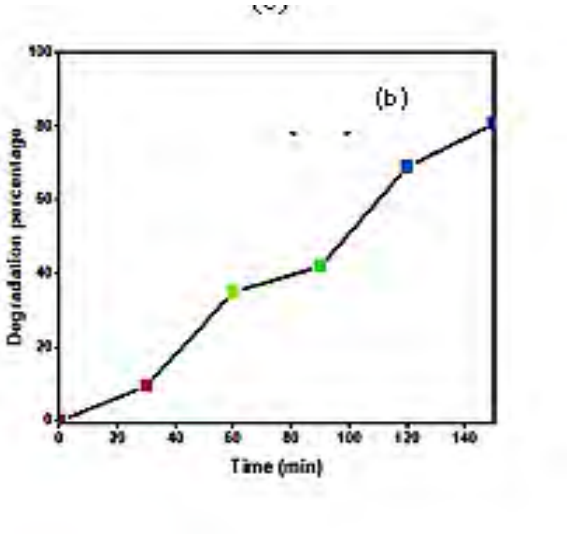

Figure 4.8 (a) Time optimization of S3. **Figure 4.8 (b) Degradation % of S3.**

48%, 68%, 81%, 84% and 91% respectively.

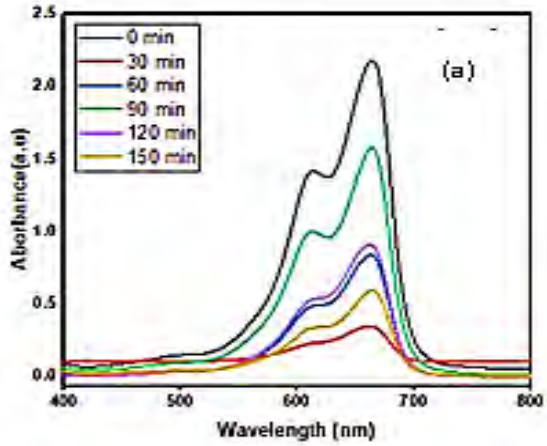

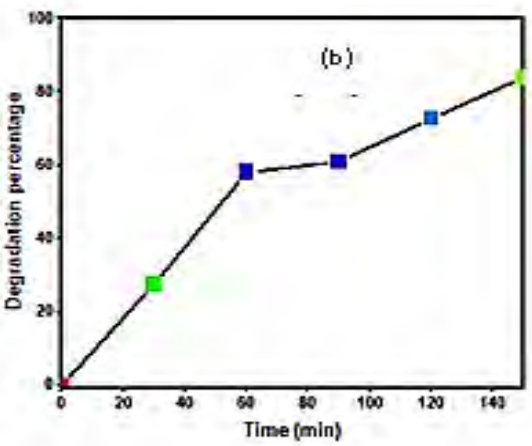

Figure 4.9 (a) Time optimization of S4. **Figure 4.9 (b) Degradation % of S4.**

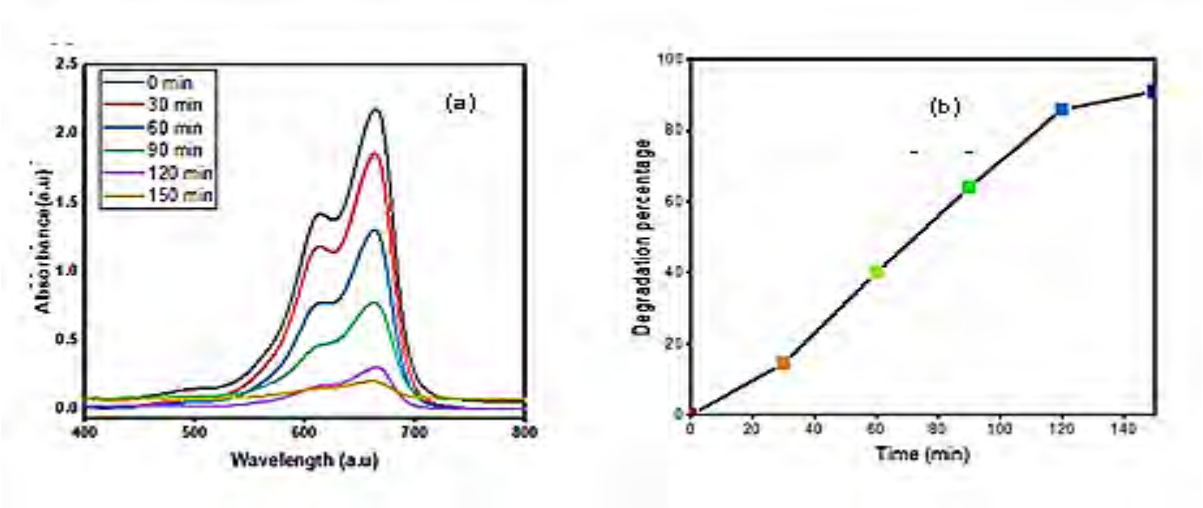

Figure 4.10 (a) Time optimization of S4. **Figure 4.10 (b) Degradation % of S5.**

4.5.2 Selection of Appropriate Photocatalyst for Methylene Blue Degradation

Five synthesized catalysts S1, S3, S4 and S5 were tested for their photocatalytic efficacy in the degradation of methylene blue using 0.04 g of each catalyst. The solutions that resulted withstood 150 minutes of visible light irradiation. Based on how well each of these five catalysts worked to degrade dye as planned, the best one was picked. We chose the (S5)(ZnO)0.60/(CuO)0.40 photocatalyst for future research of methylene blue degradation because UV absorption values and color shifts revealed that it had the greatest photocatalytic performance among the five photocatalysts.

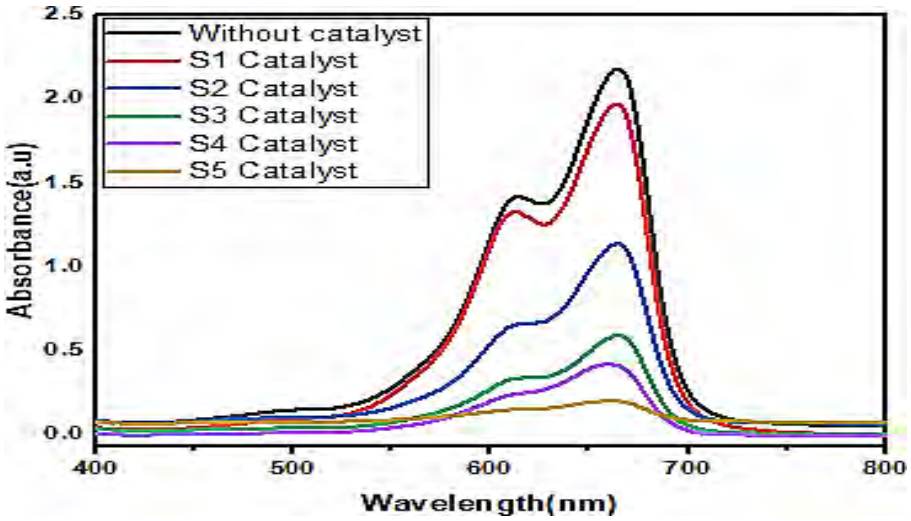

Figure 4.11 UV-Visible spectra of all samples

4.5.3 Assessment of photocatalytic activity

The photocatalytic performance of the produced samples is evaluated using the photocatalytic degradation of methylene blue dye under light irradiation. Figure 4.11 displays the photo-degradation graphs of the MB dye for each sample under equal lighting conditions. The photocatalytic activity and degradation percentage is calculated using the equations given below,

$$\textbf{Photodegradation \%} = \left(\frac{C_0 - C_i}{C_0}\right) \times 100$$

$$\textbf{Photo catalytic Activity} = C_i / C_o$$

Where Co represents the initial concentration of dye and C represents the concentration after the reaction time.

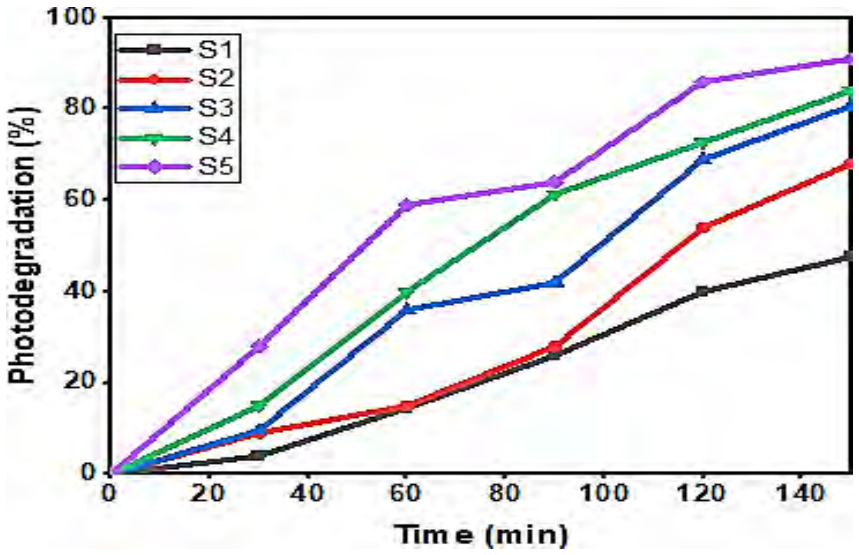

Figure 4.12 Photodegradation percentage with time.

The percentage photodegradation efficiency of S1, S2, S3, S4, and S5 at various concentrations is shown in figure 4.12. Because a large number of free radicals must be created during a redox reaction in order to degrade the dye, Pure ZnO showed a lower degradation percentage than CuO/ZnO samples, because ZnO has a wide band gap and

requires large amount of energy to jump the valence electron into the conduction band. Thus, only a few electrons are able to transit from the valence band to the conduction band when exposed to visible light, and the amount of degradation is quite little (approximately 48%). If we look at further samples that are made by coupling a low energy band gap CuO, the pohotocatalytic percentage is rising since the band gap energy is decreasing and there are a lot of more active sites available for light absorption. Thus, after 150 minutes of irradiation, S5 (ZnO) 0.60/ (CuO) 0.40 displays the largest percentage of MB dye degradation which is 91 percent.

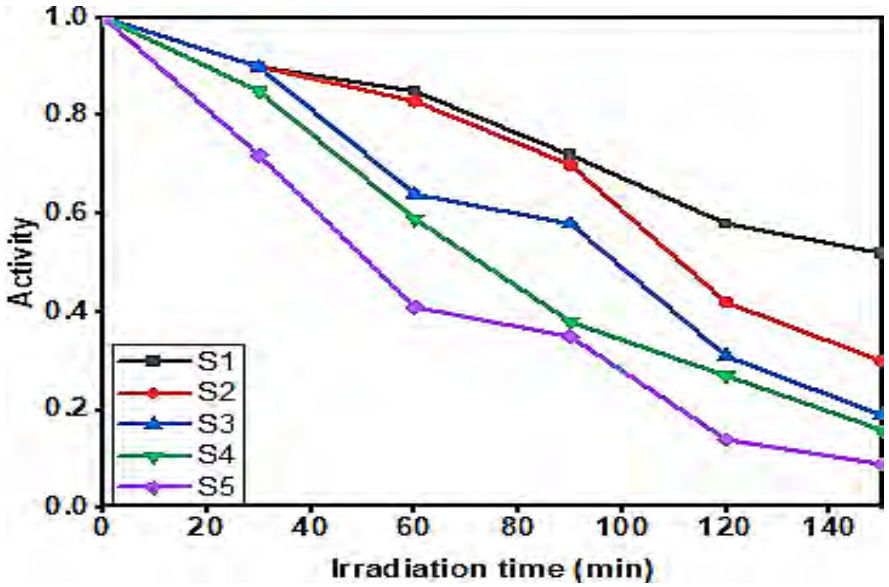

Figure 4.13 Activity of S1, S2, S3, S4 and S5.

The residual dye content is described by the activity of a sample. The figure 4.17 tells the concentration of dye content at a particular time. Here a graph is plotted for all the samples to observe the behavior of dye against each catalyst. After 150 minutes the sample S5 (ZnO) 0.60/ (CuO) 0.40 have degraded maximum dye molecules which means that it lowers the activity of methylene blue to a minimum value. This also shows that S5 is a better catalyst among all.

4.6 Conclusion

A series of samples S1,S2, S3 ,S4, and S5 was successfully prepared by CHM approach. By varying loading concentrations of CuO, the crystallite size of the samples varies from

23.44 to 8.14 nm. It has also been observed that the major peaks shift toward higher angle in S4 and S5 indicating that d-spacing is decreased. For the sample S2 major peak shifted towards lower angle due to increase in d-spacing and confirms that there is expansion occurs. An FTIR peak is observed in the range 490 to 600 cm^{-1} shows the formation of ZnO/CuO metal oxide. Moreover, optical properties have been studied by UV-Vis. Spectroscopy. Absorption coefficient and optical band gap of all samples were calculated using absorbance data. The band gap of CuO/ZnO varies from 3.22 to 1.73 eV with varying the CuO concentrations. Morphological analysis shows that the synthesized nanocomposites are cotton like porous structure with increasing porosity and surface area as we increase CuO concentration. Reasonable absorption in ZnO/CuO nanoparticles especially in the visible region authenticate their suitability as photo catalysts. From this study, we concluded that S5 Nano composites are highly photoactive than other concentrations. About 91 % dye was degraded in 150 min. The better performance of photo catalysts can be attributed to enhanced light absorption and lower electron hole recombination.

References

1. Pradeep, T., *Nano: the essentials: understanding nanoscience and nanotechnology*. 2007: McGraw-Hill Education.
2. Feynmann, R., *There's a plenty of room at the bottom, Caltech Eng*. 1960, Sci.
3. Smalley, R. *Congressional Hearings*. 1999. Summer.
4. Klabunde, K.J. and R.M. Richards, *Nanoscale materials in chemistry*. 2009: John Wiley & Sons.
5. Kiss, L., et al., *New approach to the origin of lognormal size distributions of nanoparticles.* 1999. **10**(1): p. 25.
6. Rana, S., *Environmental pollution, health and toxicology. Alpha science International Ltd*. 2006, Oxford, UK.
7. Kuriakose, S., B. Satpati, and S.J.P.C.C.P. Mohapatra, *Enhanced photocatalytic activity of Co doped ZnO nanodisks and nanorods prepared by a facile wet chemical method.* 2014. **16**(25): p. 12741-12749.
8. Lam, S.-M., et al., *Degradation of wastewaters containing organic dyes photocatalysed by zinc oxide: a review.* 2012. **41**(1-3): p. 131-169.
9. Mohammed, M., A. Shitu, and A.J.R.J.C.S.I. Ibrahim, *Removal of methylene blue using low cost adsorbent: a review.* 2014. **2231**: p. 606X.
10. Loera-Serna, S., et al., *Elimination of methylene blue and reactive black 5 from aqueous solution using HKUST-1.* 2017. **8**(4): p. 241.
11. Konstantinou, I. and T.J.E.i. Albanis, *Worldwide occurrence and effects of antifouling paint booster biocides in the aquatic environment: a review.* 2004. **30**(2): p. 235-248.
12. Chatterjee, D., S.J.J.o.P. Dasgupta, and P.C.P. Reviews, *Visible light induced photocatalytic degradation of organic pollutants.* 2005. **6**(2-3): p. 186-205.
13. Huang, C., C. Dong, and Z.J.W.m. Tang, *Advanced chemical oxidation: its present role and potential future in hazardous waste treatment.* 1993. **13**(5-7): p. 361-377.
14. González, E.S., et al. *Estudios españoles de crecimiento: situación actual, utilidad y recomendaciones de uso*. in *Anales de pediatría*. 2011. Elsevier.
15. Malik, R., V.K.J.R. Tomer, and S.E. Reviews, *State-of-the-art review of morphological advancements in graphitic carbon nitride (g-CN) for sustainable hydrogen production.* 2021. **135**: p. 110235.
16. Colmenares, J.C. and R.J.C.S.R. Luque, *Heterogeneous photocatalytic nanomaterials: prospects and challenges in selective transformations of biomass-derived compounds.* 2014. **43**(3): p. 765-778.

17. Ahmed, S., et al., *Influence of parameters on the heterogeneous photocatalytic degradation of pesticides and phenolic contaminants in wastewater: a short review.* 2011. **92**(3): p. 311-330.

18. Szczepanik, B.J.A.C.S., *Photocatalytic degradation of organic contaminants over clay- TiO2 nanocomposites: A review.* 2017. **141**: p. 227-239.

19. Umar, M., H.A.J.O.p.-m. Aziz, risk, and treatment, *Photocatalytic degradation of organic pollutants in water.* 2013. **8**: p. 196-197.

20. Masoumbeigi, H., A.J.J.o.H.P. Rezaee, and S. Health, *Removal of Methylene Blue (MB) dye from synthetic wastewater using UV/H2O2 advanced oxidation process.* 2015. **2**(1).

21. Si, Y., et al., *Photocatalytic performance of a novel MOF/BiFeO3 composite.* 2017. **10**(10): p. 1161.

22. Saravanan, R., et al., *Photocatalytic degradation of organic dye using nano ZnO.* 2011. **10**(01n02): p. 253-257.

23. Reza, K.M., A. Kurny, and F.J.A.W.S. Gulshan, *Parameters affecting the photocatalytic degradation of dyes using TiO2: a review.* 2017. **7**(4): p. 1569-1578.

24. Rajeshwar, K., et al., *Heterogeneous photocatalytic treatment of organic dyes in air and aqueous media.* 2008. **9**(4): p. 171-192.

25. Fu, M., et al., *Sol–gel preparation and enhanced photocatalytic performance of Cu- doped ZnO nanoparticles.* 2011. **258**(4): p. 1587-1591.

26. Sakib, A.A.M., et al., *Synthesis of CuO/ZnO nanocomposites and their application in photodegradation of toxic textile dye.* 2019. **3**(3): p. 91.

27. Cahino, A.M., et al., *Characterization and evaluation of ZnO/CuO catalyst in the degradation of methylene blue using solar radiation.* 2019. **45**(11): p. 13628-13636.

28. Harish, S., et al., *Controlled structural and compositional characteristic of visible light active ZnO/CuO photocatalyst for the degradation of organic pollutant.* 2017. **418**: p. 103-112.

29. Mardikar, S.P., S. Kulkarni, and P.V.J.J.o.E.C.E. Adhyapak, *Sunlight driven highly efficient degradation of methylene blue by CuO-ZnO nanoflowers.* 2020. **8**(2): p. 102788.

30. Hanif, M., et al., *Highly Efficient and Sustainable ZnO/CuO/g-C3N4 Photocatalyst for Wastewater Treatment under Visible Light through Heterojunction Development.* 2022. **12**(2): p. 151.

31. Meena, P.L., et al., *Fabrication of ZnO/CuO Hybrid Nanocomposite for Photocatalytic Degradation of Brilliant Cresyl Blue (BCB) Dye in Aqueous Solutions.* 2021. **6**(3): p. 196- 211.

32. SILVA, W.J.D., M.R. SILVA, and K.J.J.o.t.C.C.S. Takashima, *Preparation and characterization of Zno/CuO semiconductor and photocatalytic activity on the decolorization of direct red 80 azodye.* 2015. **60**(4): p. 2749-2751.

33. Sharma, R., et al., *Synthesis of magnetic nanoparticles using potato extract for dye degradation: A green chemistry experiment.* 2019. **96**(12): p. 3038-3044.

34. Chang, T., et al., *Enhanced photocatalytic activity of ZnO/CuO nanocomposites synthesized by hydrothermal method.* 2013. **5**(3): p. 163-168.

35. Taufique, M., et al., *ZnO–CuO nanocomposites with improved photocatalytic activity for environmental and energy applications.* 2018. **47**(11): p. 6731-6745.

36. Khan, T.M., et al., *Mechanisms of composite-hydroxide-mediated approach for the synthesis of functional ZnO nanostructures and morphological dependent optical emissions.* 2015. **6**: p. 592-599.

37. Pelaz, B., et al., *Diverse applications of nanomedicine.* 2017. **11**(3): p. 2313-2381.

38. Acedo-Mendoza, A., et al., *Photodegradation of methylene blue and methyl orange with CuO supported on ZnO photocatalysts: The effect of copper loading and reaction temperature.* 2020. **119**: p. 105257.

39. Xiong, G., et al., *Photoluminesence and FTIR study of ZnO nanoparticles: the impurity and defect perspective.* 2006. **3**(10): p. 3577-3581.

40. Naz, N.A., *Abdul Ghafar Wattoo, Zhenlun Song, M. Zubair Iqbal, Muhammad Rizwan, Ahmad Saeed, Sajjad Ahmad, Akbar Ali.*

41. PP, V.J.B., *In vitro biocompatibility and antimicrobial activities of zinc oxide nanoparticles (ZnO NPs) prepared by chemical and green synthetic route—A comparative study.* 2020. **10**(1): p. 112-121.

42. Acharya, K.P., *Photocurrent spectroscopy of CdS/plastic, CdS/glass, and ZnTe/GaAs hetero-pairs formed with pulsed-laser deposition*. 2009, Bowling Green State University.

43. Hameeda, B., et al., *Development of Cu-doped NiO nanoscale material as efficient photocatalyst for visible light dye degradation.* 2021. **40**(4): p. 1396-1406.